Calculation of Incompressible Rough-Wall Boundary-Layer Flows

Tuncer Cebeci* and K. C. Chang†
California State University at Long Beach, Long Beach, Calif.

The algebraic eddy viscosity model of Cebeci and Smith has been modified to account for wall roughness by incorporating a suggestion of Rotta. The boundary-layer equations are solved, with this model, by the accurate and efficient Keller Box scheme for a wide variety of experimental configurations. These include adverse, zero, and favorable pressure gradients, and roughness elements that approach the upper limits of Rotta's model. Comparison of calculated and measured values of skin friction and integral thickness confirms the applicability of the procedure for all cases presented.

Nomenclature

A = Van Driest damping length or constant in the law of wall
b = $1+\epsilon_m^+$
c_f = local skin-friction coefficient $\tau_w/\frac{1}{2}\rho u_e^2$
k = roughness height
k_s = equivalent sand roughness
k_s^+ = $k_s u_\tau/\nu$
L = spacing between roughness elements
ℓ = mixing length
m_1 = $\frac{1}{2}(1+m_2)$
m_2 = pressure gradient parameter $(x/u_e)(du_e/dx)$
R_x = Reynolds number $u_e x/\nu$
s = length of roughness element
u,v = components of velocity in x and y directions
x,y = Cartesian coordinates
ϵ_m = eddy viscosity
ϵ_m^+ = dimensionless eddy viscosity ϵ_m/ν
ν = kinematic viscosity
ρ = density
κ = Prandtl's constant, 0.41
λ = roughness density L/s
δ = boundary-layer thickness
δ^* = displacement thickness $\int_0^\infty [1-(u/u_e)]dy$
θ = momentum thickness $\int_0^\infty (u/u_e)[1-(u/u_e)]dy$
τ_w = wall shear stress

Subscripts

0 = parameters evaluated at y_0
e = edge conditions
w = wall conditions
$(\,)'$ = differentiation with respect to η

I. Introduction

TWO possible approaches to the calculation of the properties of turbulent boundary-layer flow over rough surfaces are exemplified by the integral method of Dvorak[1] and the differential method of Antonio and Wood.[2] The former is based on the procedure of Head[3] and the latter on that of Bradshaw et al.[4] In both cases, the assumptions used to characterize the turbulent flow were modified to represent the influence of the rough wall. The integral equations are complemented by auxiliary relationships, and the equation used for the drag coefficient was altered. For the differential method, the finite-difference equations are linked to the wall by an empirical function adjusted to account for roughness.

The relative advantages of differential methods have become increasingly apparent in recent years and are made more obvious by the adjustment necessary to the drag law of Head's procedure. The differential approach of Bradshaw et al. makes use of a turbulence energy equation with assumptions that allow the solution of hyperbolic equations; it was tested, with near-wall modifications, for their new experimental data by Antonio and Wood. Their measurements were obtained in the vicinity of a rough wall made up of nearly square cavities and steps and in a zero-pressure-gradient flow.

The present calculated results were obtained with the numerical scheme of Cebeci and Keller which has been used for several boundary-layer applications and is described in detail by Cebeci and Bradshaw.[5] For smooth-wall flows, it has made use of the effective-viscosity hypothesis of Cebeci and Smith,[6] and this is extended here to represent flow over rough walls without and with pressure gradients. The procedure solves one fewer equation than that of Bradshaw et al. and is based on the Keller Box scheme, which allows particularly accurate and economical solutions to the differential equations. The near-wall modification to the procedure, which is necessary to account for the influence of roughness, may be related to that of Antonio and Wood and is based on the earlier contribution of Rotta.[7]

Calculations are performed for the experimental configurations of Ardnt and Ippen,[8] Bettermann,[9] Coleman et al.,[10] Liu et al.,[11] Perry and Joubert,[12] Pimenta et al.,[13] and Scottron and Power[14] which encompass three-dimensional and two-dimensional rough elements, with a range of roughness density from 2 to 12 and freestream velocity distributions corresponding to adverse, zero, and favorable pressure gradients. The equivalent sand roughnesses vary from $k_s^+ \approx 20$ to k_s^+ about 2000, the upper limit of Rotta's displaced model. These data were chosen partly because they provide a particularly useful range of geometries and freestream conditions and partly because the flow profile parameters required to generate initial data are available at upstream stations, thus eliminating uncertainties associated with the estimation of initial conditions.

The present paper is intended to be brief, and, as a consequence, the following section states but does not discuss the equations, turbulence model, and numerical scheme; the near-wall modification is described, in slightly more detail, in that section. Results, a short discussion, and summary conclusions are presented in the third and final sections.

Received Jan. 6, 1978; revision received April 17, 1978.

Index category: Boundary Layers and Convective Heat Transfer—Turbulent.

*Distinguished Professor, Mechanical Engineering Department. Member AIAA.

†Research Associate, Mechanical Engineering Department.

II. Equations and Solution Procedure

The equations representing conservation of mass and momentum in a two-dimensional, incompressible, boundary-layer flow may be written as

$$\frac{\partial u}{\partial x}+\frac{\partial v}{\partial y}=0 \tag{1}$$

$$u\frac{\partial u}{\partial x}+v\frac{\partial u}{\partial y}=u_e\frac{\mathrm{d}u_e}{\mathrm{d}x}+\frac{\partial}{\partial y}\left[\nu\frac{\partial u}{\partial y}-\overline{u'v'}\right] \tag{2}$$

Before we solve Eqs. (1) and (2), we use the Falkner-Skan transformation with a similarity parameter

$$\eta=\sqrt{u_e/\nu x}\,y \tag{3a}$$

and a dimensionless stream function $f(x,\eta)$ defined by

$$\psi=\sqrt{u_e\nu x}\,f(x,\eta) \tag{3b}$$

Together with the definition of eddy viscosity, with primes denoting differentiation with respect to η, we can write Eqs. (1) and (2) as

$$(bf'')'+m_1ff''+m_2[1-(f')^2]=x\left(f'\frac{\partial f'}{\partial x}-f''\frac{\partial f}{\partial x}\right) \tag{4}$$

Here the definitions of parameters b, m_1, and m_2 are given in the Nomenclature.

The eddy-viscosity formulation of Cebeci and Smith[6] is used here and provides separate equations for the outer and inner layers. In the outer region,

$$(\epsilon_m)_0=0.0168\left|\int_0^\infty(u_e-u)\,\mathrm{d}y\right| \tag{5a}$$

and in the inner region,

$$(\epsilon_m)_i=\ell^2\left|\frac{\partial u}{\partial y}\right| \tag{5b}$$

with

$$\ell=0.4y[1-\exp(-y/A)] \tag{6a}$$

$$A=26\nu u_\tau^{-1}\Big/\left(1-11.8\frac{\nu u_e}{u_\tau^3}\frac{\mathrm{d}u_e}{\mathrm{d}x}\right)^{1/2} \tag{6b}$$

In terms of the transformed variables, Eqs. (5) and (6) become

$$\epsilon_m^+=\begin{cases}0.16R_x^{1/2}\eta^2|f''|[1-\exp(-y/A)]^2\\ 0.0168R_x^{1/2}(\eta_e-f_e)\end{cases} \tag{7}$$

where

$$\frac{y}{A}=\frac{\eta R_x^{1/4}|f_w''|^{1/2}}{26}[1-11.8m_2R_x^{-1/4}|f_w''|^{-3/2}]^{1/2}$$

The expression for $(\epsilon_m)_i$ is modified to represent the influence of surface roughness with the help of Rotta's model,[7] which recognizes that the velocity profiles for smooth and rough walls can be similar, provided that the coordinates are displaced; we rewrite ℓ in Eq. (6) as

$$\ell=0.4(y+\Delta y)\{1-\exp[-(y+\Delta y)/A]\} \tag{8}$$

and express Δy as a function of an equivalent sand-grain roughness parameter $k_s^+(\equiv k_su_\tau/\nu)$, i.e.,

$$\Delta y=0.9(\nu/u_\tau)[\sqrt{k_s^+}-k_s^+\exp(-k_s^+/6)] \tag{9}$$

This expression is valid for $4.535<k_s^+<2000$, with the lower limit corresponding to the upper bound for hydraulically smooth surface.

It remains to provide a link between k_s^+ and the geometry of a particular rough surface. Schlichting[15] has determined experimentally equivalent sand roughness for a large number of roughnesses arranged in a regular fashion. Dvorak[1] has established a correlation between the velocity shift Δu_l and the roughness density λ for two-dimensional rectangular rough elements from which the equivalent sand roughness can be determined (for detail, see Cebeci and Bradshaw[5]). For the roughness elements other than the ones investigated by Schlichting and Dvorak, the equivalent sand roughness must be determined experimentally or by some empirical methods.

The solution of Eq. (4) requires initial conditions as well as boundary conditions. For a laminar flow, there is no difficulty with the initial conditions, since they can be obtained easily by solving Eq. (4) at $x=0$. On the other hand, when the flow is turbulent, the generation of initial conditions is not that easy. In our study, we made use of the modified version of Coles' velocity profile[5,6]:

$$\frac{u}{u_\tau}=2.44\left[\ell n\frac{yu_\tau}{\nu}+\left(\frac{y}{\delta}\right)^2\left(1-\frac{y}{\delta}\right)+\Pi\left(1-\cos\pi\frac{y}{\delta}\right)+B_l(k_s^+)\right] \tag{10a}$$

and applied it to flows on both smooth and rough walls in the region $\epsilon<y\le\delta$. Here ϵ is the virtual origin defined as $(u/u_\tau)_{y=\epsilon}=0.0$. The function $B_l(k_s^+)$ is given by Eq. (15). For a given c_f and R_θ, the boundary-layer thickness δ and the wake parameter Π are determined from the following expressions:

$$\frac{\kappa\delta^*u_e}{\delta u_\tau}=\frac{11}{12}+\Pi(1-2\epsilon^*)+\epsilon^*(\ell n\epsilon^*-1.0) \tag{10b}$$

$$\frac{\kappa^2(\delta^*-\theta)u_e^2}{\delta u_\tau^2}=1.9123+[3.056+4\epsilon^*(\ell n\epsilon^*-1.0)]\Pi+(1.5-4\epsilon^*)\Pi^2 \tag{10c}$$

$$\kappa u_e/u_\tau=\ell n\delta^+ +B_l+2\Pi \tag{10d}$$

where

$$\epsilon^*=\epsilon/\delta,\qquad \delta^+=\delta u_\tau/\nu,\qquad \kappa=0.41$$

The usual boundary conditions for Eqs. (1) and (2) are

$$y=0,\quad u=0,\quad v=0 \tag{11a}$$

$$y=\delta,\quad u=u_e(x) \tag{11b}$$

In terms of transformed variables defined by Eq. (3), Eq. (11) becomes

$$\eta=0,\quad f'=0,\quad f=0 \tag{12a}$$

$$\eta=\eta_e,\quad f'=1 \tag{12b}$$

For turbulent flows, it is sometimes more convenient to use "wall" boundary conditions at some distance y_0 away from the wall. Usually this y_0 is taken to be the distance, given by

$$y_0=(\nu/u_\tau)y_0^+$$

with y_0^+ given by 50 for smooth surfaces. In that case, the "wall" boundary conditions for u and v can be represented by

$$u_0 = u_\tau \left[\frac{1}{\kappa} \ell n \frac{y_0 u_\tau}{\nu} + C + \frac{2}{\kappa} \ell n \left\{ \frac{2}{1+\sqrt{1+z}} + \sqrt{1+z} - 1 \right\} \right] \quad (13a)$$

$$v_0 = -\frac{u_0 y_0}{u_\tau} \frac{du_\tau}{dx} \quad (13b)$$

Here C is a constant equal to 5.2, and

$$u_\tau^2 = \frac{\tau_0}{\rho} - \alpha y_0, \quad \alpha = 0.3 \frac{du_0^2}{dx} - u_e \frac{du_e}{dx}, \quad z = \frac{\alpha y_0}{u_\tau^2} \quad (14)$$

For flows over rough walls we shall use Eqs. (13a) and (13b), except now C in Eq. (13a) is replaced by $B_1(k_s^+)$. This function is given by[5]

$$B_1 = 5.2; \qquad k_s^+ < 2.25 \quad (15a)$$

$$B_1 = 5.2 + [8.5 - 5.2 - (1/\kappa) \ell n\, k_s^+] \sin[0.4258(\ell n\, k_s^+ - 0.811)];$$

$$2.25 \le k_s^+ \le 90 \quad (15b)$$

$$B_1 = 8.5 - (1/\kappa) \ell n\, k_s^+, \qquad k_s^+ > 90 \quad (15c)$$

In terms of transformed coordinates, the boundary conditions Eqs. (13a) and (13b), become

$$\eta = \eta_0, \qquad (f_0')^2 = \alpha_1 f_0'' - \gamma_1 \quad (16a)$$

$$2x \frac{\partial f_0}{\partial x} + (1+m_2) f_0 = \eta_0 f_0' \left[(1-m_2) + \frac{x}{u_\tau^2} \frac{du_\tau^2}{dx} \right] \quad (16b)$$

where

$$\alpha_1 = \frac{B^2}{R_x^{1/2}} b_0, \quad \gamma_1 = \frac{\alpha y_0}{u_e^2} B^2 \quad (17a)$$

$$B = \frac{1}{\kappa} \ell n \frac{y_0 u_\tau}{\nu} + B_1(k_s^+) + \frac{2}{\kappa} \left(\ell n \frac{2}{1+\sqrt{1+z}} + \sqrt{1+z} - 1 \right) \quad (17b)$$

with B_1 being equal to C for a smooth wall and being equal to the expression given by Eq. (15) for a rough wall.

The solution of Eq. (4) subject to the boundary conditions given either by Eq. (12a) or Eqs. (16) and (12b) is obtained by using Keller's Box method, discussed in detail by Cebeci and Bradshaw.[5] When wall boundary conditions, Eqs. (16a) and (16b), were used, appropriate modifications were made to the solution algorithm described by Cebeci and Bradshaw.[5]

III. Results and Discussion

The numerical scheme and the eddy-viscosity formulation for flows over smooth walls have been well demonstrated by Cebeci and Smith[6] and Cebeci and Bradshaw[5] for two-dimensional plane and axisymmetric flows, as well as three-dimensional flows. Here we report the calculation of flows over rough walls in comparison with experimental data to demonstrate further that they are equally accurate for flows over rough walls.

Figure 1 presents measured values of momentum thickness, displacement thickness, and skin-friction coefficients, reported by Bettermann, together with lines corresponding to the present calculations. The measurements correspond to values of roughness density of 2.65 to 4.18 and roughness height between 0.5 and 1.5 mm. The equivalent sand roughness heights were calculated as described in Sec. II based on the correlated results presented by Dvorak.[1] The measured c_f and R_θ at the 0.4-m station, where initial perturbations have died down, were used to generate initial data. As can be seen, the agreement is generally very good, with the maximum discrepancy in skin-friction coefficient and integral thicknesses amounting to approximately 5% and corresponding to the results obtained with the longest roughness height.

The influence of pressure gradient on rough-wall boundary layer was examined experimentally by Scottron and Power. Their rough wall was formed with a square mesh screen made from 0.105-in.-diam wire with a 0.5-in. pitch in both directions. The zero-pressure-gradient experiments are represented by Figs. 2a and 2b and the agreement with calculation is excellent. Two adverse pressure gradients were used; the results of Fig. 2c correspond to the milder gradient and those of Fig. 2d to the severe gradient. As can be seen, the calculated results for the mild gradient are in good agreement with measurements, with the possible exception of the skin-friction coefficient, for which experimental discrepancies (between hot-wire and pitot-tube-type measurements) are shown to be large. In the case of the severe pressure gradient, the integral thicknesses, particularly displacement thickness, are underestimated by the calculation, but detailed

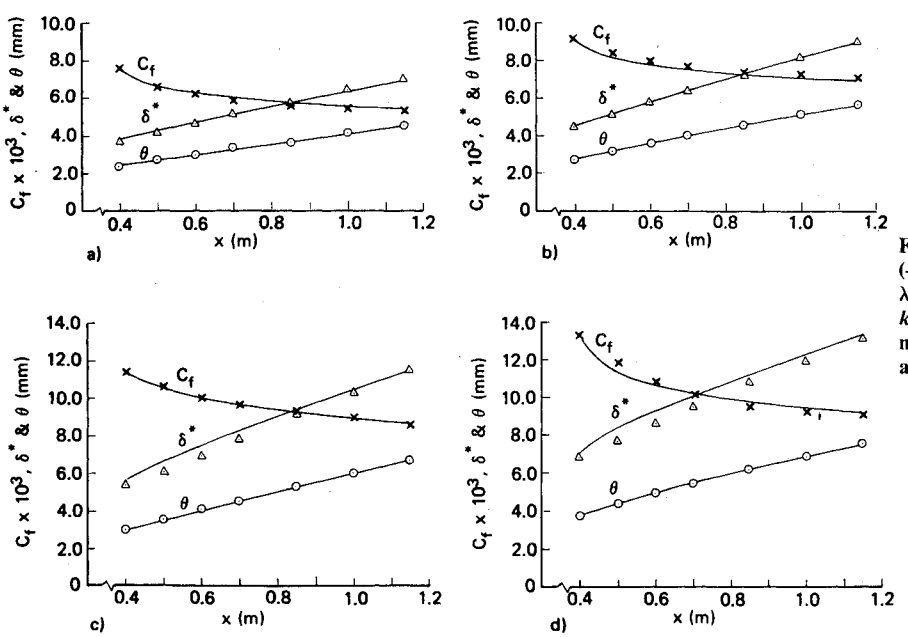

Fig. 1 Results for Bettermann's data (—computed, × △ ○ data): a) $k = 3$ mm, $\lambda = 2.65$, $k_s = 1.26$ mm; b) $k = 3$ mm, $\lambda = 3.30$, $k_s = 3.8$ mm; c) $k = 2.4$ mm, $\lambda = 4.13$, $k_s = 9.26$ mm; d) $k = 4.0$ mm, $\lambda = 4.18$, $k_s = 14.0$ mm. In all cases, $u_e = 30$ m/s, $\nu = 1.44 \times 10^{-5}$ m^2/s.

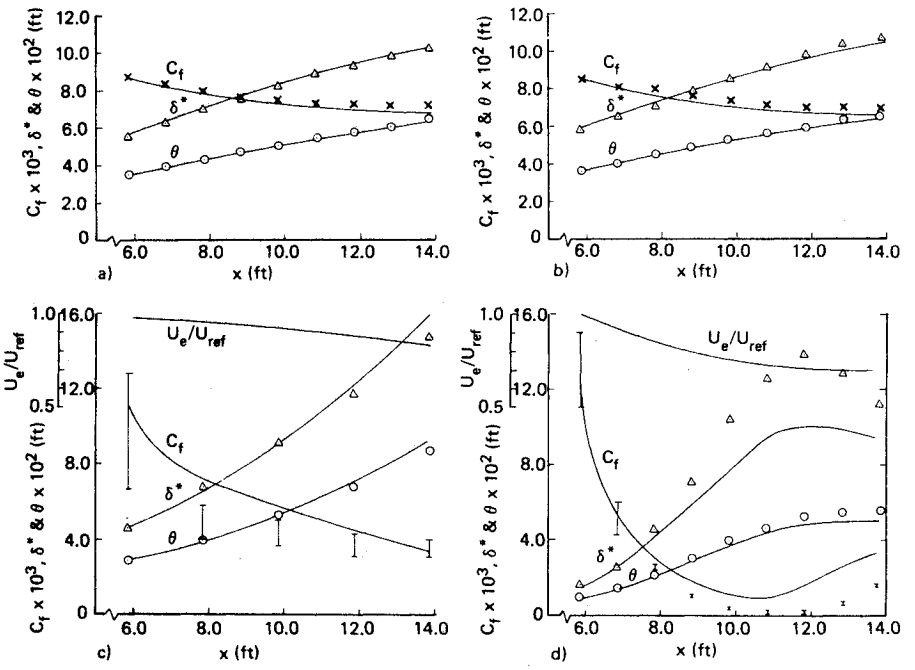

Fig. 2 Results for Scottron and Power's data (——computed, × △ ○ data): a) $u_e = 37$ ft/s; b) $u_e = 68$ ft/s; c) mild adverse pressure gradient; d) strong adverse pressure gradient. In all cases $k = 0.0175$ ft, $\lambda = 3.7$, $k_s = 0.039$ ft, $\nu = 1.61 \times 10^{-4}$ ft^2/s, $u_{ref} = 100$ ft/s.

tests for three-dimensionality were not repeated and could account for at least part of the discrepancy. Another possible reason may be the inaccuracy of reading experimental freestream velocity distribution from the small graph given by Scottron and Power.

Perry and Joubert's data serve as another test for flows over rough walls with adverse pressure gradient. They measured the boundary layers in a closed-circuit-type wind tunnel over rough surface made of 0.125-in.-square bar elements with roughness density of 4 held to the plate by strips of double-coated adhesive tape. Because of difficulty in accurately determining c_f for flows with pressure gradients from the measured velocity profiles based on Clauser's plot, they deduced the wall shear stress based on Coles' wake function. In general, the agreement between the calculated and experimental results is good, as shown in Fig. 3.

Liu et al. measured the flows in a circulated water channel over a family of flat surfaces with transverse roughness elements made of 0.250 ± 0.01-in.-square bars with roughness density ranging from 2 to 12. All flows have zero pressure gradients and 0.5-ft/s freestream velocity. For $\lambda = 4.0$ and 12.0, the equivalent sand roughness were determined based on Dvorak's correction. For $\lambda = 2.0$, the experimental value was used because Dvorak's correction predicted too low a value. The resulting values of k_s^+ range from 20 to over 100, with Reynolds numbers based on momentum thickness being below 2000. Thus these experimental data serve as a good test for low Reynolds number, transition, and roughness-density effects on the turbulent-flow modeling. The computed results in comparison with the experimental data are shown in Fig. 4. The integral thicknesses are in good agreement with the computed and experimental data, whereas the computed skin-friction coefficients deviate from the experimental data, with a maximum difference about 10%.

The results of Arndt and Ippen[8] differ from those mentioned in previous paragraphs. They were obtained with triangular grooves of height 0.1, 0.05, 0.025, and 0.0125 in.; the peak-to-peak distance between each groove was equal to twice the roughness height. This geometrical arrangement is not represented by the equivalent sand roughness based on Dvorak's correlation, and, for the present calculations, the measured relationships of Arndt and Ippen were employed. The calculated results for the three smaller roughness heights which fall within the acceptable limits of the present Rotta-type near-wall method, are shown on Fig. 5. The freestream

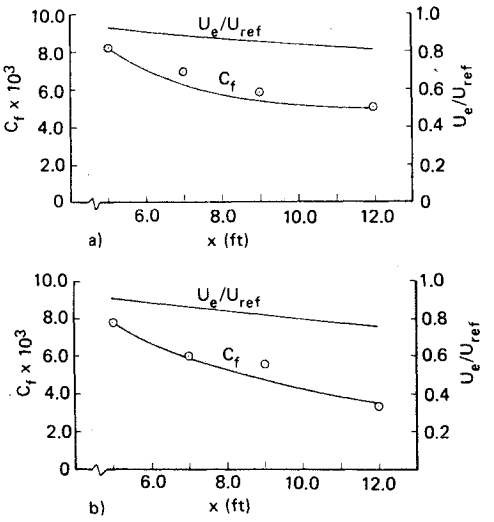

Fig. 3 Results for Perry and Joubert's data for two different external velocity distributions (——computed, ○ data). In both cases, $k = 0.0104$ ft, $\lambda = 4.0$, $k_s = 0.0346$ ft, $\nu = 1.56 \times 10^{-4}$ ft^2/s, $u_{ref} = 100$ ft/s.

velocities are essentially uniform, although significant experimental scatter exists. The results are again in excellent agreement.

The roughness elements used by Pimenta et al.[13] and Coleman et al.[10] again are different from the previous ones. They measured the flows on rough surfaces composed of densely packed spheres of uniform size with a diameter of 0.05 in. This arragement is the same as the one used by Schlichting in pipe flows. The equivalent sand roughness height ($\equiv 1.25r$, with r denoting the radius of the roughness element) suggested by Schlichting then was used in the present calculations. Pimenta et al. considered the flows on a flat plate, as did Coleman et al., who also investigated favorable pressure gradients on both equilibrium and nonequilibrium flows; both authors also studied the heat transfer and transpiration on rough surfaces. The present results and the experimental data are presented in Figs. 6 and 7. For flows with zero pressure gradient, good agreement again is observed. For flows with strong favorable pressure gradients, the computed results are somewhat higher than the experimental data.

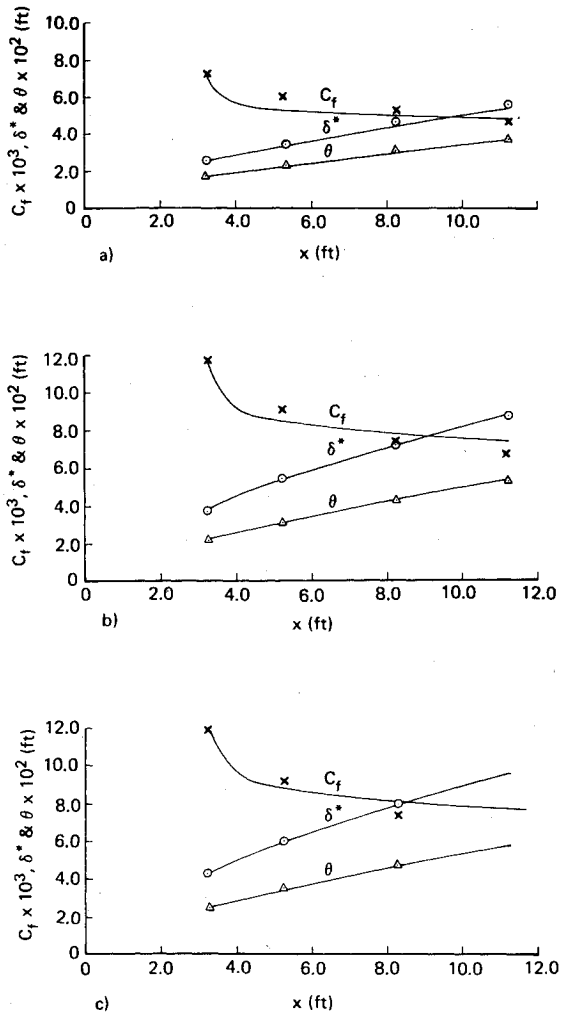

Fig. 4 Results for Liu et al. data (—computed, × △ ○ data): a) $k = 0.0208$ ft, $\lambda = 2.0$, $k_s = 0.01$ ft; b) $k = 0.0208$ ft, $\lambda = 4.0$, $k_s = 0.0455$ ft; c) $k = 0.0208$ ft, $\lambda = 12.0$, $k_s = 0.0572$ ft. In all cases, $u_e = 0.5$ ft/s, $\nu = 1.04 \times 10^{-5}$ ft^2/s.

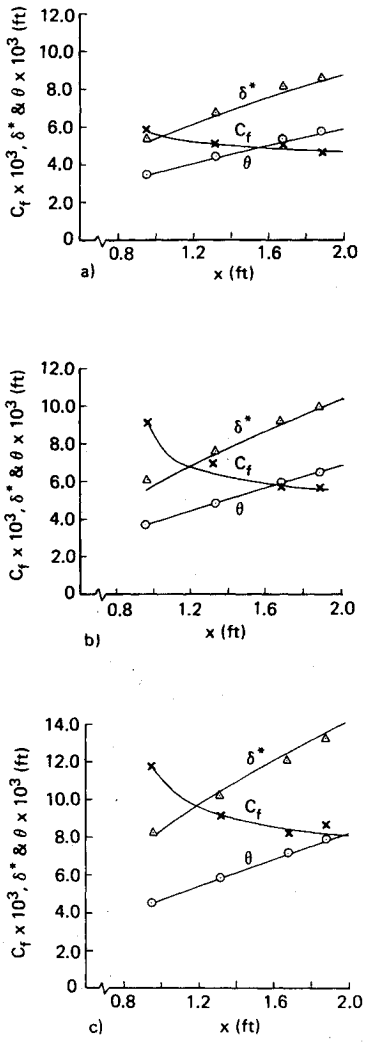

Fig. 5 Results for Arndt and Ippen's data (—computed, × △ ○ data): a) $k_s = 0.001$ ft; b) $k_s = 0.0023$ ft; c) $k_s = 0.0082$ ft. In all cases, $u_e = 40.25$ ft/s, $\nu = 0.95 \times 10^{-5}$ ft^2/s.

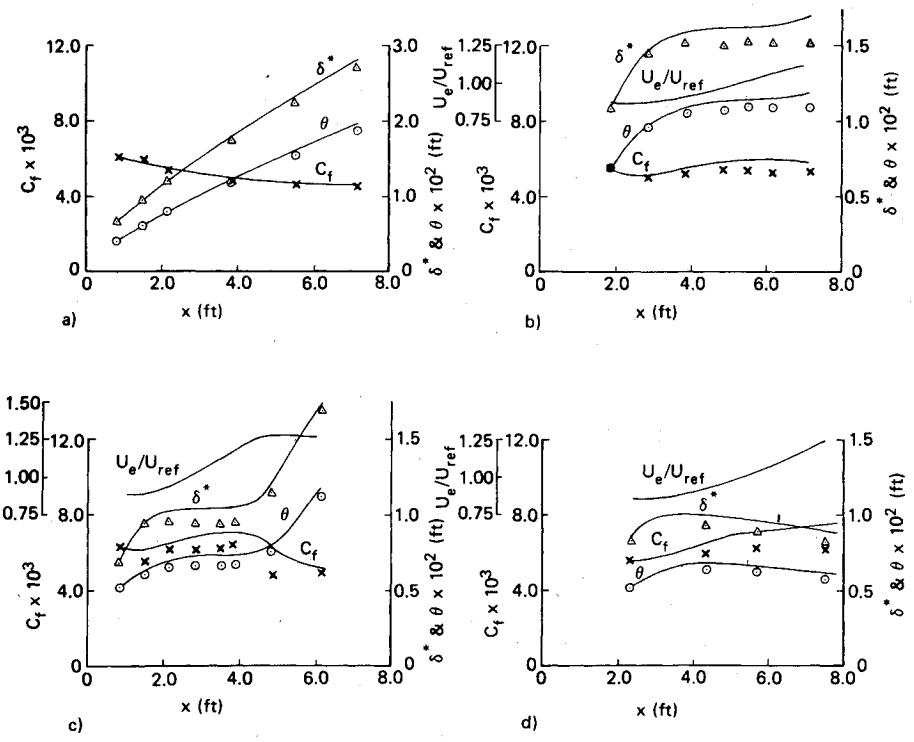

Fig. 6 Results for Coleman et al.'s data (— computed, × △ ○ data): a) $u_e = 86.7$ ft/s; b) and c) equilibrium flow with strong favorable pressure gradient; d) nonequilibrium flow with strong favorable pressure gradient. In all cases, $k = 0.0042$ ft, $k_s = 0.0026$ ft, $\nu = 1.63 \times 10^{-4}$ ft^2/s.

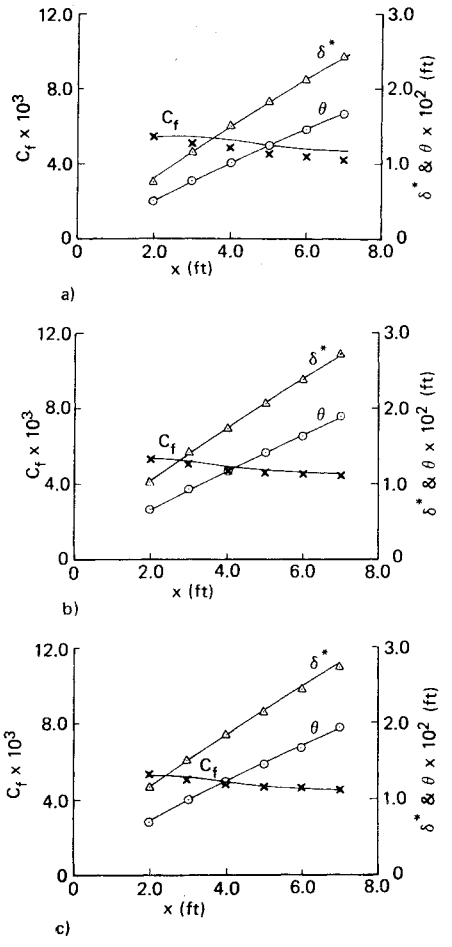

Fig. 7 Results for Pimenta et al.'s data (——computed, × △ ○ data): a) $u_e = 52$ ft/s; b) $u_e = 89$ ft/s; c) $u_e = 130$ ft/s. In all cases, $k = 0.0042$ ft, $k_s = 0.0026$ ft, $\nu = 1.61 \times 10^{-4}$ ft^2/s.

IV. Concluding Remarks

In general, the comparisons of the previous sections indicate that the influence of roughness on the properties of boundary-layer flow can be calculated with the procedure of Sec. II. The measurements allow an appraisal over a limited range of roughness geometries and pressure gradients and neither represent a complete spectrum of likely geometries nor provide, in all cases, necessary accuracy. Nevertheless, for many design purposes, the comparisons provide the necessary assurance that the method is adequate for their purposes, at least within the stated range of validity of the Rotta model and, where information of the equivalent sand-grain roughness is not provided, within the range of applicability of Dvorak's correlation.

Acknowledgment

This work was supported by the Office of Naval Research under Contract N00014-77-C-0156.

References

[1] Dvorak, F. A., "Calculation of Turbulent Boundary Layers on Rough Surfaces in Pressure Gradient," *AIAA Journal*, Vol. 7, Sept. 1969, pp. 1752-1759.

[2] Antonia, R. A. and Wood, D. H., "Calculation of a Turbulent Boundary Layer Downstream of a Small Step Change in Surface Roughness," *Aeronautical Quarterly*, Vol. 26, Aug. 1975, pp. 202-210.

[3] Head, M. R., "Entrainment in the Turbulent Boundary Layer," Aeronautical Research Council, R&M 3152, 1958.

[4] Bradshaw, P., Ferriss, D. H., and Atwell, A. N., "Calculation of Turbulent Boundary-Layer Development Using the Turbulent Energy Equation," *Journal of Fluid Mechanics*, Vol. 28, May 1967, pp. 593-616.

[5] Cebeci, T. and Bradshaw, P., *Momentum Transfer in Boundary Layers*, Hemisphere Publishing Co., Washington, D.C., 1977.

[6] Cebeci, T. and Smith, A. M. O., *Analysis of Turbulent Boundary Layers*, Academic Press, New York, 1974.

[7] Rotta, J. C., "Turbulent Boundary Layers in Incompressible Flow," *Progress in Aerospace Science*, Vol. 2, 1962, pp. 1-219.

[8] Arndt, R. E. A. and Ippen, A. T., "Cavitation Near Surfaces of Distributed Roughness," Hydrodynamics Lab., Dept. of Civil Engineering, Massachusetts Inst. of Technology, Rept. 104, 1967.

[9] Bettermann, D., "Contribution a l'Etude de la Couche Limite Turbulente le long de la Plaques Rugueuses," Centre National de la Recherche Scientifique, Paris, Rept. 65-6, 1965.

[10] Coleman, H. W., Moffat, R. J., and Kays, W. M., "Momentum and Energy Transport in the Accelerated Fully Rough Turbulent Boundary Layer," Dept. of Mechanical Engineering, Stanford Univ., Stanford, Calif., Rept. HMT-24, 1976.

[11] Liu, C. K., Kline, S. J., and Johnston, J. P., "An Experimental Study of Turbulent Boundary Layer on Rough Walls," Dept. of Mechanical Engineering, Stanford Univ., Stanford, Calif., Rept. MD-15, 1966.

[12] Perry, A. E. and Joubert, P. N., "Rough-Wall Boundary Layers in Adverse Pressure Gradients," *Journal of Fluid Mechanics*, Vol. 17, Oct. 1963, pp. 193-211.

[13] Pimenta, M. M., Moffat, R. J., and Kays, W. M., "The Turbulent Boundary Layer: An Experimental Study of the Transport of Momentum and Heat with the Effect of Roughness," Dept. of Mechanical Engineering, Stanford Univ., Stanford, Calif., Rept. HMT-21, 1975.

[14] Scottron, V. E. and Power, J. L., "The Influence of Pressure Gradient on the Turbulent Boundary Layer over a Rough Surface," Navy Dept., David Taylor Model Basin, Rept. 2115, 1965.

[15] Schlichting, H., *Boundary-Layer Theory*, McGraw-Hill, New York, 1968.